

# Synthesis of CeO<sub>2</sub> nano-aggregates of complex morphology

E. Mercadelli<sup>a,\*</sup>, G. Ghetti<sup>a,b</sup>, A. Sanson<sup>a</sup>, R. Bonelli<sup>b</sup>, S. Albonetti<sup>b</sup>

<sup>a</sup>*Institute of Science and Technology for Ceramics, National Research Council, CNR-ISTEC, Via Granarolo 64, I-48018 Faenza, Italy*

<sup>b</sup>*Department of Industrial Chemistry and Materials (INSTM, Research Unit of Bologna), University of Bologna, Viale Risorgimento 4, 40136 Bologna, Italy*

Received 1 June 2012; received in revised form 22 June 2012; accepted 22 June 2012

Available online 7 July 2012

## Abstract

Cerium oxide with spheric, flowerlike and needle-like shapes has been synthesized by a simple microwave assisted method using diethylene glycole in mild conditions. The effect of reaction temperature on the crystal structure and morphology were thoroughly discussed. The structural evolutions and morphological characteristics of the nanostructures were investigated using X-ray diffractometry, scanning and transmission electron microscopy, Fourier transform infrared spectroscopy, TGA/DSC and BET analysis. By changing experimental conditions pure CeO<sub>2</sub> fluoritic phase or cerium formate with complex morphology were formed. High porosity CeO<sub>2</sub> nanostructures, retaining the end-reaction morphology, were readily obtained by calcination of cerium precursor. This simple and economic soft chemical method leads to nanostructured–micrometric aggregates of cerium oxide with high specific surface area suitable for catalytic applications.

© 2012 Elsevier Ltd and Techna Group S.r.l. All rights reserved.

**Keywords:** A. Powders: chemical preparation; D. CeO<sub>2</sub>; Nanostructures; Catalytic properties

## 1. Introduction

Cerium oxide is a rare earth oxide that has attracted a great interest due to some unique properties, such as oxygen storage capacity and conductivity, high UV absorption and hardness and stability at high temperatures [1]. As a consequence, CeO<sub>2</sub> has been widely used for catalysis [2–4], fuel cells [5] and sensors [6].

The physical/chemical properties of cerium oxides are strongly dependent on their microstructures, including size, morphology, and specific surface area [7]; therefore, the preparation of nanocrystalline ceria has been drawing much attention by the material scientists and chemists.

A variety of chemical techniques have been utilized to prepare ceria nanomaterials, including hydrothermal [8–10], microemulsion [11–13], precipitation [14,15], sol–gel [16–18], and solvothermal synthesis [19–21].

The polyol-mediated technique, is a simple chemical synthesis that directly precipitates highly pure mixed oxides [22], and a variety of other materials, including sulfides and phosphates [23] in a high-boiling alcohol. In this procedure,

“polyol” stands as a general term for polyalcohols with high boiling temperature and ability to solve inorganic salts. The polyol method is generally applied for the preparation of metal particles mainly for its mild reducing properties. However polyalcohols can also be exploited for their chelating effect that avoids the particles agglomeration during synthesis. In the case of oxides, the polyol method can then be considered as a precipitation process carried out at elevated temperatures with an accurate control of particle growth [24]. Due to its high dipole moment, the polyol can also serve as an excellent solvent for microwave heating; microwave-polyol method is in fact a promising method for rapid preparation of nanomaterials [25]. Compared to the conventional one, microwave dielectric heating has some unique advantages for the synthesis of nanostructured materials, such as the rapid volumetric heating which causes a fast homogeneous nucleation that in some cases leads to the formation of novel nanostructures [26].

In this study, the synthesis parameters were carefully tailored in order to control the reaction mechanism and the final powder morphology. Cerium oxide powders of different morphology were successfully prepared by microwave irradiation under mild conditions. The effect of reaction temperature and used solvent on the crystal structure and morphology

\*Corresponding author. Tel.: +39 054 669 9743; fax: +39 056 446 381.

E-mail address: [elisa.mercadelli@istec.cnr.it](mailto:elisa.mercadelli@istec.cnr.it) (E. Mercadelli).

were discussed. A combination of high surface area and rods-like morphology was found to favor the efficiency of ceria catalysts for the total oxidation of toluene.

## 2. Experimental

Cerium nitrate hexahydrate ( $\text{Ce}(\text{NO}_3)_3 \cdot 6\text{H}_2\text{O}$ , 99.5%, Aldrich) was used as starting material. The cerium nitrate was dispersed in diethylene glycol (DEG) to have a final cerium concentration of 0.1 M. The solution was heated under reflux in a commercial microwave oven designed for chemical synthesis (MicroSYNTH Plus, Milestone) at the final temperature for 2 h. To improve the hydrolysis of the cerium salt, a water excess ( $[\text{Ce}^{3+}]:[\text{H}_2\text{O}]=1:10$ ) was added to the DEG solution at 140 °C. The precipitated powders were separated by centrifugation, washed in ethanol and characterized by X-ray diffraction. XRD measurements were carried out at room temperature with a Bragg/Brentano diffractometer (X'PertPro PANalytical) equipped with a fast X'Celerator detector, using Cu anode as X-ray source ( $K\alpha$ ,  $\lambda=1.5418 \text{ \AA}$ ). Thermogravimetry (TG) and Differential Scanning Calorimetry (DSC) were carried out in air flux at a heating rate of 10 °C/min using a simultaneous thermal analyzer (STA 449, Netzsch, Selb/Bavaria). Infrared spectra were recorded in the range from 400 to 4000  $\text{cm}^{-1}$ , using a Fourier transform infrared spectrometer (FTIR) (Perkin-Elmer 1700). The powder morphology was investigated by scanning electron microscopy (SEM, Leica Cambridge Stereoscan 360) and transmission electron microscope (TEM, Philips CM 100). The specific surface area of the calcined powders was measured by the BET method (Sorptly 1750, Carlo Erba). Catalytic experiments were carried out in a fixed bed glass reactor at atmospheric pressure. A K-type thermocouple was placed into the catalyst bed to monitor the reaction temperature. Each run used approximately 350 mg of catalyst in the form of 30–60 mesh (250–595  $\mu\text{m}$ ) particles, mixed with 1120 mg of corundum grains of similar size for better temperature control. The total volumetric flow through the catalyst bed was held constant at 140  $\text{ml min}^{-1}$ , 10 vol% oxygen, 90 vol% nitrogen and 1400 ppm of toluene. Analyses of reactants and products were carried out as follows: the products in the outlet stream were scrubbed in cold acetone maintained at –25 °C by a F32 Julabo Thermostat. Analysis of reactants and products were carried out with a GC Clarus 500 (Perkin-Elmer) equipped with a Elite FFAP column (30 m  $\times$  0.32 mm) and a FID. CO and  $\text{CO}_2$  formed were separated on a capillary column Elite Plot Q (30 m  $\times$  0.32 mm), attached to a methanizer and analyzed with a flame ionization detector (FID). Particular care was devoted to the determination of the C balance, which was found to always fall between 95% and 105% (calculated as the comparison between converted toluene and the sum of the product yields).

## 3. Results and discussion

Nanocrystalline ceria particles were produced by one-step microwave-assisted synthesis from a diethylene glycol solution

of cerium nitrate adjusting the synthesis conditions. In particular, the effect of the temperature on the formation of the fluoritic phase was carefully studied synthesizing powders at four different temperatures between 140 and 180 °C.

The diffractograms of the as-prepared powders (Fig. 1) show a drastic effect of the reaction temperature on the nature and number of the phases formed. In particular, a mix of phases ( $\text{CeO}_2/\text{Ce}(\text{COOH})_3$ ) is produced for temperatures higher than 160 °C, while nanocrystalline pure cerium oxide is obtained at 140 °C.

This behavior is probably due to a series of complex redox equilibria involving cerium, nitrates and glycol as indicated in Fig. 2.

Below 160 °C, in fact, the oxidant power of the nitrates promotes the oxidation of Ce (III) of the precursor salt; at this stage, the  $\text{H}_2\text{O}$  added reacts with Ce (IV) causing the nucleation of  $\text{CeO}_2$ . For temperatures between 140 and 160 °C, the Ce (III) is completely oxidized to  $\text{CeO}_2$  by the nitric part of the precursor. This was confirmed by the evolution of red-brown gases from the reaction vessel. At  $T \geq 160 \text{ °C}$  the  $\text{NO}_3^-$  species still present induce the glycol oxidation leading to the formation of carboxylic acids and finally formic acid (Fig. 3) as already reported by Shen and Ruest [27] and Ho et al. [28]. Temperatures above 160 °C triggers the DEG reduction capability [29,30]; assuming that all the nitrates are eliminated as  $\text{NO}_x$ , the glycol starts to reduce the Ce (IV) back to Ce (III). Finally, the latter is complexed by the formic acid, by-product of the DEG oxidation, leading to a mix of phases ( $\text{CeO}_2/\text{Ce}(\text{COOH})_3$ ).

This hypothesis was supported by FTIR results obtained on samples synthesized at different temperatures (Fig. 4). Besides

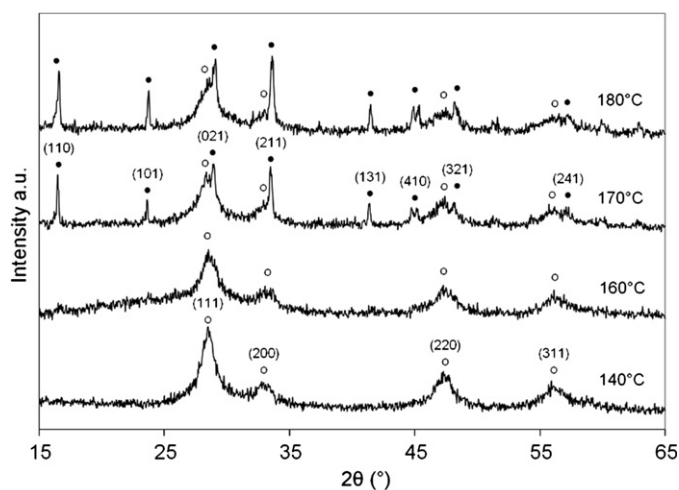


Fig. 1. Influence of the synthesis temperatures on XRD patterns of the as prepared ceria samples. o= $\text{CeO}_2$  (JCPDF 34-384), and ●= $\text{Ce}(\text{COOH})_3$  (JCPDF 49-1245).



Fig. 2. Scheme of the hypothetical cerium redox behavior during the synthesis at different temperatures.

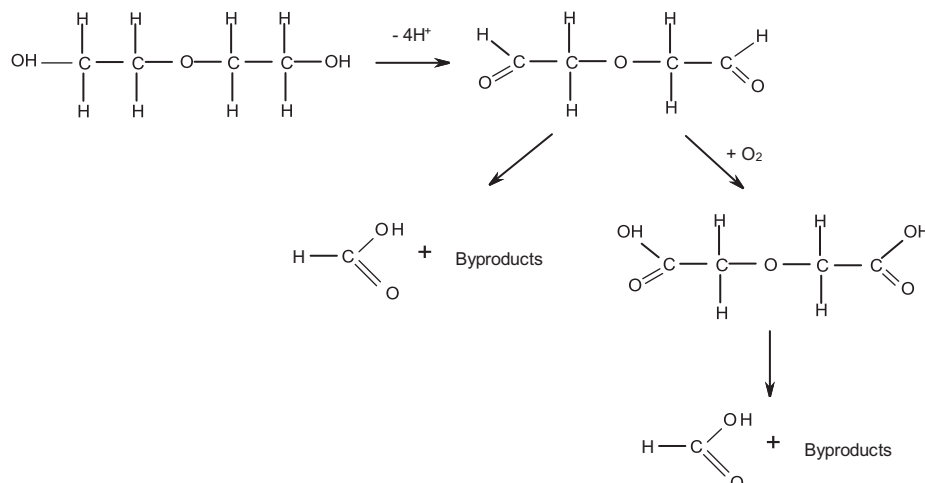


Fig. 3. Reaction scheme of DEG oxidation.

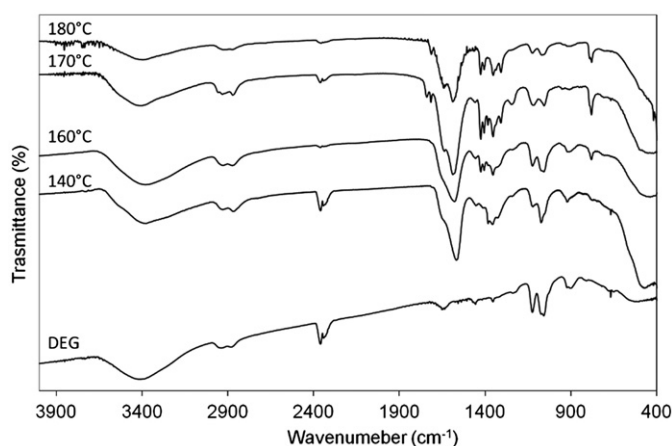


Fig. 4. Influence of the synthesis temperatures on FTIR spectra of the as-prepared ceria samples.

the characteristic peaks related to the DEG adsorption, the spectra of the as-synthesized powders show peaks related to the DEG decomposition by-products. In particular for the samples synthesized at higher temperatures, a band related to the O–C=O bending that could be associated to the formate species can be identified at  $780\text{ cm}^{-1}$ . Moreover, the band observed at  $500\text{--}400\text{ cm}^{-1}$  and related to the metal–oxygen bond, is more intense for the sample synthesized at lower temperatures indicating a higher amount of ceria formed.

Fig. 5(a) and (b) show respectively TG and DSC analyses carried out in air flux for the as-prepared powders synthesized at different temperatures. The lowest weight loss (15%) is detected for the sample synthesized at  $140^\circ\text{C}$  while the highest one (25%) is related to the powder obtained at  $180^\circ\text{C}$ . Moreover, the loss of weight observed for materials synthesized at  $170^\circ\text{C}$  and  $180^\circ\text{C}$  was shifted to higher temperatures, indicating the presence of different compounds in these two samples in respect of the others obtained at lower temperatures. On the basis of XRD results the observed weight losses can be assigned either to the decomposition of DEG (or its

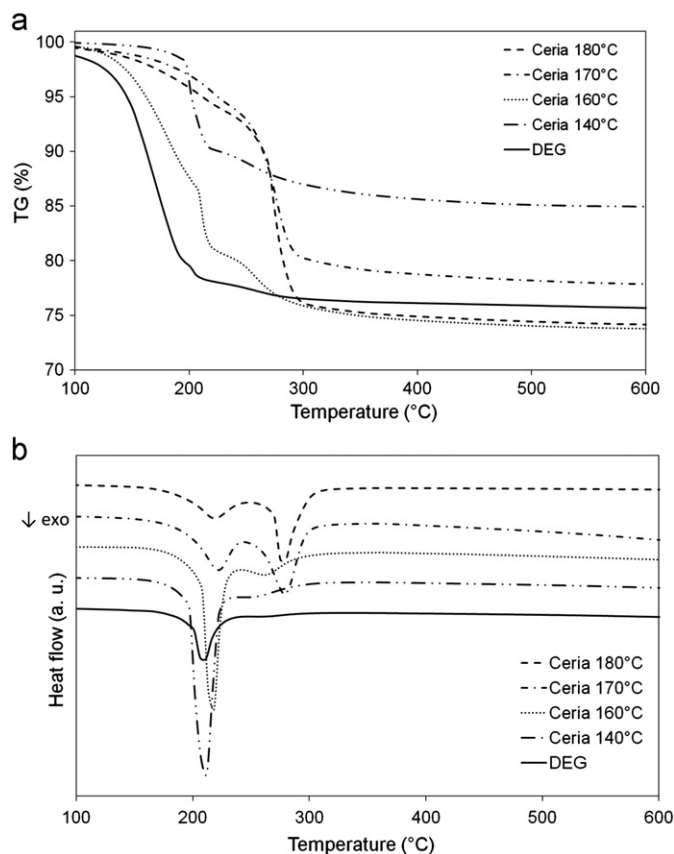


Fig. 5. Synthesis temperature effect on the thermal evolution of the as-synthesized powders: (a) TG curves, and (b) DSC curves.

derivates) adsorbed onto the powders surface and/or to the formate combustion. The thermal profiles showed by the DSC curves of powders synthesized at  $170^\circ\text{C}$  and  $180^\circ\text{C}$  show two exothermic peaks, centered at  $220$  and  $280^\circ\text{C}$ , that can be linked to the residual-DEG combustion and to cerium formate decomposition, respectively.

In order to verify this assumption, TG–DSC analyses on pure  $\text{CeO}_2$  powders impregnated with the glycol were

recorded. These analyses confirmed a decomposition temperature of 220 °C for DEG as before asserted.

The conversion of  $\text{Ce}(\text{COOH})_3$  to  $\text{CeO}_2$  at 280 °C was confirmed comparing the weight loss associated at that temperature with the theoretical weight loss value needed to transform the amount of cerium-formate phase determined by XRD, into cerium oxide. On the other hand only the peak associated to the DEG combustion is detected for the powders synthesized at lower temperatures, confirming XRD results.

The average crystallite size of the powders synthesized at the lowest temperature (140 °C) was estimated by the XRD patterns, using Debye–Scherrer equation. The average crystallite size of 5–6 nm calculated from the diffractograms was confirmed also by TEM analysis (Fig. 6).

The morphological analysis of the powders synthesized at different temperatures are reported in Fig. 7. The pure  $\text{CeO}_2$  powders show a spherical shape, while the presence

of  $\text{Ce}(\text{COOH})_3$  as secondary phase induces the formation of more complex morphologies (flowerlike and needle-like shapes). This behavior has been observed by Ho et al. [28] and linked to a bridging behavior typical of the of the formate species.

A calcination treatment at 400 °C is needed both for converting the  $\text{Ce}(\text{COOH})_3$  into the pure fluoritic phase and to completely remove the organic residues adsorbed on the surface of all samples. This thermal treatment does not influence the powders morphology indicating that the pure nanocrystalline ceria can be obtained with different morphologies tuning the  $\text{Ce}(\text{COOH})_3/\text{CeO}_2$  ratio.

The specific surface area values of the different calcined samples are reported in Fig. 8. The high surface area (140–170  $\text{m}^2/\text{g}$ ) of the samples synthesized at high temperatures can be related to the different morphologies induced by

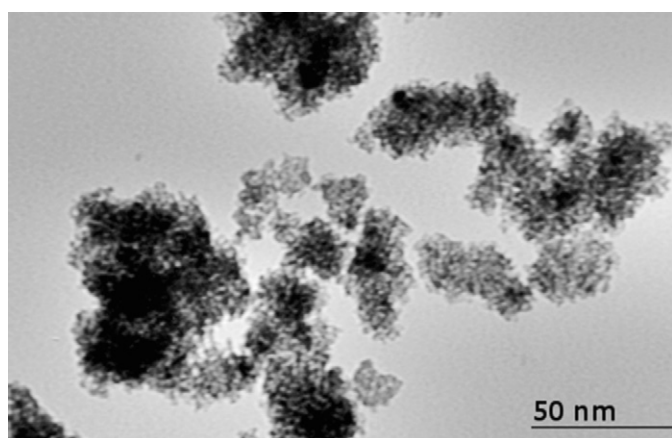


Fig. 6. TEM micrograph of pure nano-ceria synthesized at 140 °C.

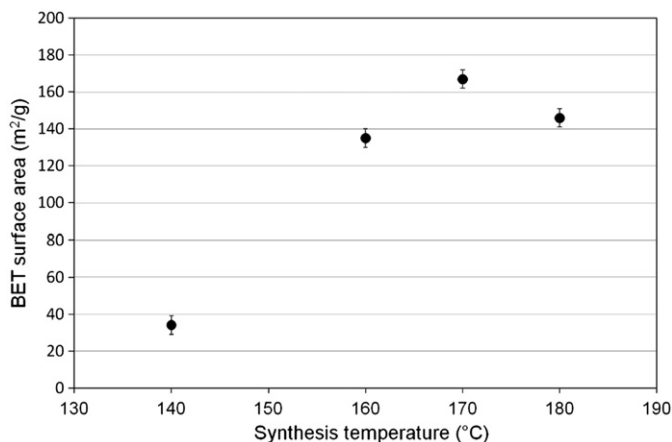


Fig. 8. BET surface area measured after calcination at 400 °C of ceria synthesized at different temperatures.

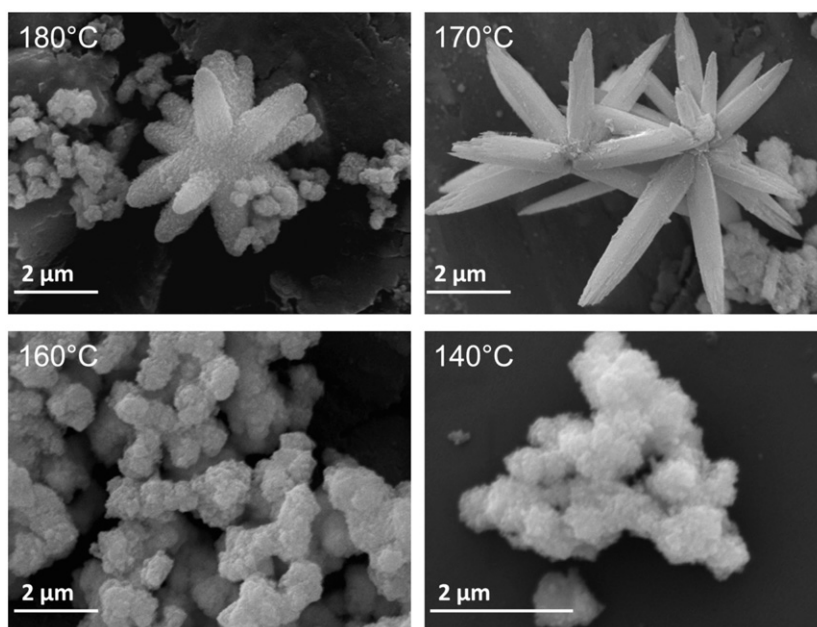


Fig. 7. SEM micrographs of as prepared ceria samples at different temperatures.



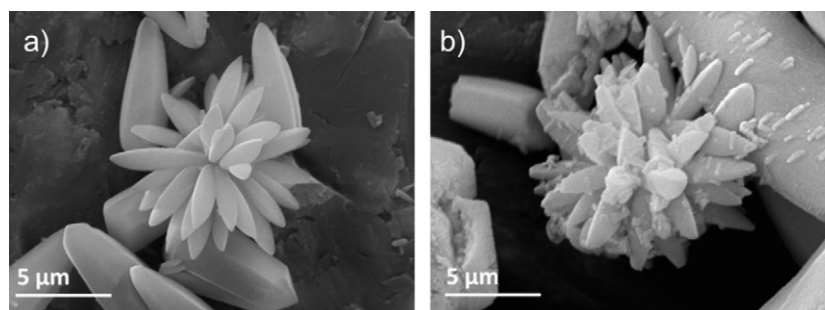


Fig. 9. SEM micrographs of powders: (a) as-prepared and (b) as-calcined at 400 °C.

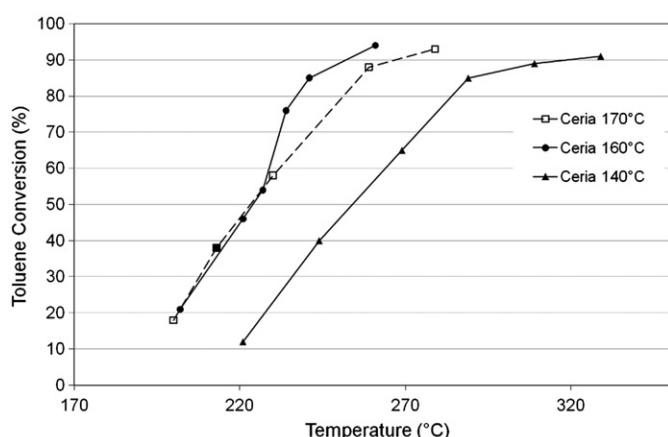


Fig. 10. Catalytic activity for the combustion of toluene of powders synthesized at different temperatures.

the presence of  $\text{Ce}(\text{COOH})_3$ . The micrometric particles of cerium formate produced at temperatures above 160 °C, are transformed into cerium oxides during the calcination step. The  $\text{CO}_2$  evolution, associated to this phase conversion, leads to the formation of mesoporous aggregates with high specific surface area which retain the complex morphology (Fig. 9).

Nano-crystalline ceria catalysts prepared by microwave-assisted reaction were tested for the total oxidation of toluene, as probe molecule of model aromatic hydrocarbons (Fig. 10). High catalytic activity was observed for all samples at relatively low temperature and no formation of partial oxidation products was revealed,  $\text{CO}_2$  being the only detected product in the range of investigated temperatures. Nevertheless, the catalytic performances of these samples were found to be different, depending, as expected, on surface area, morphology and crystallite size of the  $\text{CeO}_2$  powders.  $\text{CeO}_2$  powders derived from the complex morphology show a higher efficiency for toluene removal than the others materials, probably due to their highly porous structure. Combining a high surface area with micrometric aggregate dimension could be a key point for obtaining powders with high catalytic properties and easy handling. The as-prepared ceria can be considered as a promising material for environmental applications able to link a high efficiency to an easy handling and processing.

#### 4. Conclusions

Nanocrystalline ceria particles were successfully produced by one-step microwave-assisted synthesis from a glycol solution of metal nitrates under mild conditions. The as-prepared powder showed a good crystallinity and nanometric particle size. Moreover, by adjusting the synthesis conditions, micrometric nanostructured ceria of complex morphology and high specific surface area can also be obtained.

This simple and economic soft chemical method leads to directly obtain nanometric cerium oxide with a high specific surface area suitable for catalytic applications.

#### References

- [1] A. Trovarelli, *Catalysis by Ceria and Related Materials*, Imperial College Press, London, 2002.
- [2] E. Aneggi, M. Boaro, C. De Leitenburg, G. Dolcetti, A. Trovarelli, Insights into the redox properties of ceria-based oxides and their implications in catalysis, *J. Alloys Compd.* 408 (2008) 1096–1102.
- [3] E.N. Ndiyor, T. Garcia, B. Solsona, S.H. Taylor, Influence of preparation conditions of nano-crystalline ceria catalysts on the total oxidation of naphthalene, a model polycyclic aromatic hydrocarbon, *Appl. Catal. B* 76 (2007) 248–256.
- [4] Tana, M. Zhang, J. Li, H. Li, Y. Li, W. Shen, Morphology-dependent redox and catalytic properties of  $\text{CeO}_2$  nanostructures: nanowires, nanorods and nanoparticles, *Catal. Today* 148 (2009) 179–183.
- [5] G.M. Christie, F.P.F. Van Berkel, Microstructure-ionic conductivity relationships in ceria-gadolinia electrolytes, *Solid State Ionics* 83 (1996) 17–27.
- [6] P. Jasinski, T. Suzuki, H.U. Anderson, Nanocrystalline undoped ceria oxygen sensor, *Sens. Actuators B* 95 (2003) 73–77.
- [7] J. Li, G. Lu., H. Li, Y. Wang, Y. Guo, Y. Guo, Facile synthesis of 3D flowerlike  $\text{CeO}_2$  microspheres under mild condition with high catalytic performance for CO oxidation, *J. Colloid Interface Sci.* 360 (2011) 93–99.
- [8] Y.C. Zhou, M.N. Rahaman, Hydrothermal synthesis and sintering of ultrafine  $\text{CeO}_2$  powders, *J. Mater. Res.* 8 (2003) 1680–1686.
- [9] R. Srivastava, Eco-friendly and morphologically-controlled synthesis of porous  $\text{CeO}_2$  microstructure and its application in water purification, *J. Colloid Interface Sci.* 348 (2010) 600–607.
- [10] C.S. Pan, D.S. Zhang, L.Y. Shi, CTAB assisted hydrothermal synthesis, controlled conversion and CO oxidation properties of  $\text{CeO}_2$  nanoplates, nanotubes, and nanorods, *J. Solid State Chem.* 181 (2008) 1298–1306.

- [11] T. Masui, K. Fujiwara, K.I. Machida, G.Y. Adachi, T. Sakata, H. Mori, Characterization of cerium(IV) oxide ultrafine particles prepared using reversed micelles, *Chem. Mater.* 9 (1997) 2197–2204.
- [12] M. Sanchez-Dominguez, L.F. Liotta, G. Di Carlo, G. Pantaleo, A.M. Venezia, C. Solansa, M. Boutonnet, Synthesis of  $\text{CeO}_2$ ,  $\text{ZrO}_2$ ,  $\text{Ce}_{0.5}\text{Zr}_{0.5}\text{O}_2$ , and  $\text{TiO}_2$  nanoparticles by a novel oil-in-water microemulsion reaction method and their use as catalyst support for CO oxidation, *Catal. Today* 158 (2010) 35–43.
- [13] E. Kockrick, C. Schrage, A. Grigas, D. Geiger, S. Kaskel, Synthesis and catalytic properties of microemulsion-derived cerium oxide nanoparticles, *J. Solid State Chem.* 181 (2008) 1614–1620.
- [14] M. Ozawa, Effect of oxygen release on the sintering of fine  $\text{CeO}_2$  powder at low temperature, *Scr. Mater.* 50 (2004) 61–64.
- [15] J. Rebellato, M.M. Natile, A. Glisenti, Influence of the synthesis procedure on the properties and reactivity of nanostructured ceria powders, *Appl. Catal. A* 339 (2008) 108–120.
- [16] B. Ksapabutr, E. Gulari, S. Wongkasemjit, Sol-gel derived porous ceria powders using cerium glycolate complex as precursor, *Mater. Chem. Phys.* 99 (2006) 318–324.
- [17] B. Bakiz, F. Guinneton, J.P. Dallas, S. Villain, J.R. Gavarri, From cerium oxycarbonate to nanostructured ceria: relations between synthesis, thermal process and morphologies, *J. Cryst. Growth* 310 (2008) 3055–3061.
- [18] C. Laberty-Robert, J.W. Long, E.M. Lucas, K.A. Pettigrew, R.M. Stroud, M.S. Doescher, D.R. Rolison, Sol-gel-derived ceria nanoarchitectures: synthesis, characterization, and electrical properties, *Chem. Mater.* 18 (2006) 50–58.
- [19] E. Verdon, M. Devalette, G. Demazeau, Solvothermal synthesis of cerium dioxide microcrystallites: effect of the solvent, *Mater. Lett.* 25 (1995) 127–131.
- [20] M. Zawadzki, Preparation and characterization of ceria nanoparticles by microwave-assisted solvothermal process, *J. Alloys Compd.* 454 (2008) 347–351.
- [21] S. Hosokawa, K. Shimamura, M. Inoue, Solvothermal synthesis of ceria nanoparticles with large surface areas, *Mater. Res. Bull.* 46 (2011) 1928–1932.
- [22] C. Feldmann, H.O. Jungk, Polyol-mediated preparation of nanoscale oxide particles, *Angew. Chem. Int. Ed.* 40 (2001) 359–362.
- [23] C. Feldmann, C. Metzmacher, Polyol mediated synthesis of nanoscale MS particles ( $M=\text{Zn}, \text{Cd}, \text{Hg}$ ), *J. Mater. Chem.* 11 (2001) 2603–2606.
- [24] L. Poul, S. Ammar, N. Jouini, F. Fievet, F. Villain, Synthesis of inorganic compounds (metal, oxide and hydroxide) in polyol medium: a versatile route related to the sol-gel process, *J. Sol-Gel Sci. Technol.* 26 (2003) 261–265.
- [25] A. Gondolini, E. Mercadelli, A. Sanson, S. Albonetti, L. Dubova, S. Boldrini, Microwave-assisted synthesis of gadolinia-doped ceria powders for solid oxide fuel cells, *Ceram. Int.* 37 (2011) 1423–1426.
- [26] H. Yang, C. Huang, A. Tang, X. Zhang, W. Yang, Microwave-assisted synthesis of ceria nanoparticles, *Mat. Res. Bull.* 40 (2005) 1690–1695.
- [27] C.Y. Shen, D.A. Ruest, Production of diglycolic acid by nitric acid oxidation of diethylene glycol, *Ind. Eng. Chem. Process Des. Dev.* 19 (1980) 401–404.
- [28] C. Ho, J.C. Yu, T. Kwong, A.C. Mak, S. Lai, Morphology-controllable synthesis of mesoporous  $\text{CeO}_2$  nano- and micro-structures, *Chem. Mater.* 17 (2005) 4514–4522.
- [29] T. Yu, J. Joo, Y.I. Park, T. Hyeon, Large-scale nonhydrolytic sol-gel synthesis of uniform-sized ceria nanocrystals with spherical, wire, and tadpole shapes, *Angew. Chem. Int. Ed.* 44 (2005) 7411–7414.
- [30] S. Wang, F. Gu, C. Li, H. Cao, Shape-controlled synthesis of  $\text{CeOHCO}_3$  and  $\text{CeO}_2$  microstructures, *J. Cryst. Growth* 307 (2007) 386–394.